Retrofitting a Geothermal Plant with Solar and Storage to Increase Power Generation

Joshua McTigue,[1] Jose Castro,[2] Greg Mungas,[3] Nick Kramer,[3] John King,[3] Craig Turchi,[1] Guangdong Zhu [1*]

[1] National Renewable Energy Laboratory, Golden, Colorado

[2] Coso Operating Company, California

[3] Hyperlight Energy, California

** Corresponding author: Guangdong.Zhu@nrel.gov*

Keywords

Geothermal, concentrating solar, thermal energy storage, hybrid plant

ABSTRACT

Solar hybridization using concentrating solar power (CSP) can be an effective approach to augmenting the power generation and cycle efficiency of a geothermal power plant which exploits a resource with a declining fluid mass. Thermal storage can further increase the dispatchability of a geothermal/solar hybrid system, which is particularly valued for a regional grid with high renewable penetration. A hybrid plant design with thermal storage is proposed based on the requirements of the Coso geothermal field in China Lake, California. This study models one Coso plant turbine running at a load that is about 7.5 MW_e less than the design load of 30 MW_e. The objective is to increase the power production by 4 MW_e. In this system, a portion of the injection brine is heated with the solar heat-transfer fluid, before being mixed with the production well fluids. In the solar heating loop, the brine should be heated to at least 155°C to increase the net power. The solar field and storage were sized based on solar data for China Lake. Thermal storage is used to store excess power at the high solar-irradiation hours and generate additional power during the evenings. The solar-field size, type and capacity of thermal storage, and operating temperatures are critical factors in determining the most economic hybrid system. Further investigations are required to optimize the hybrid system and evaluate its economic feasibility.

1. Introduction

The productivity of a geothermal power plant typically declines over its lifetime as the geothermal resource is exploited. This may be the result of the pressure, temperature, and/or

mass flow rate of the production fluids decreasing depending on the individual field and well characteristics. Not only does the power output decrease, but in addition, the power block operates at off-design conditions, thereby reducing the system efficiency still further.

By retrofitting a geothermal plant with an additional thermal input, such as concentrating solar power (CSP), the plant can be brought closer to the design operating point so that the increased plant efficiency can further enhance power production. The use of thermal storage can allow solar power to be produced throughout the night, or to deliver additional power during times of peak demand rather than only when solar irradiation is available.

The first geothermal/solar hybrid plant was developed at the Stillwater Power Plant, Nevada, and began operation in 2015. A solar field of parabolic trough collectors supplies 17 MW_{th} of thermal power to the 33 MW_e geothermal power plant and augments production by 2 MW_e (Wendt & Mines 2015). The Stillwater plant also includes a 26 MW photovoltaic solar array, which was designed to offset the decrease in power generation that occurs at high ambient temperatures (Dimarzio *et al*. 2015). The optical performance of the solar collectors was characterized in (Zhu & Turchi 2017). Most previous studies have investigated hybrid plants with parabolic trough collectors and have not implemented thermal storage. Researchers have investigated systems using binary plants (Zhou *et al*. 2013; Ayub *et al.* 2015) and single-/double-flash plants (Lentz & Almanza 2006; Handal *et al*. 2007; Alvarenga *et al*. 2008; Miguel Cardemil *et al*. 2016).

The integration of the solar and geothermal systems is typically determined by the geothermal power plant. For instance, Handal *et al.* considered four methods for adding solar heat to the Ahuachapán geothermal field in El Salvador (Handal *et al*. 2007). Heating the brine directly from the production well was ruled out because it required a larger heat exchanger. In a subsequent paper, Alvarenga *et al.* discussed two of these methods (Alvarenga *et al.* 2008). In the first approach, brine from the first separator is heated by thermal input from a solar field in a heat exchanger (HX) and the generated steam enters the high-pressure turbine. This approach was reportedly tested successfully. In the second approach, the brine from the second flash stage is heated in the solar HX, and the lower-pressure steam enters the low-pressure turbine stage. The objective was to increase the power output of the field from 95 MW_e to 97 MW_e. The authors estimated that adding 2–3 MW_e would require a solar field of around 30 acres that delivers a heat-transfer fluid at 225°C.

Miguel Cardemil *et al.* compared adding solar heat at two locations in single- and double-flash plants in the Atacama Desert, Chile (Miguel Cardemil *et al*. 2016). After the flash tank, the solar field could either superheat the steam, or evaporate the brine. Using 2nd Law analysis, it was concluded that superheating the steam was slightly more efficient because the turbine operated more efficiently with dry steam. Double flash systems were also found to be preferable to single flash plants.

In this paper, the impact of hybridizing a geothermal field with a CSP plant and thermal storage is investigated. A hybrid plant design is developed based on the requirements of an existing geothermal field in China Lake, California. The solar-thermal input is delivered by linear Fresnel reflector technology developed by Hyperlight Energy. The existing geothermal plant is first described, followed by a discussion of the design constraints and requirements for the hybrid plant. Having selected a promising hybrid-plant design, we then investigate the influence of a

number of key variables. The final section of the paper considers the sizing and performance of the solar field and thermal storage.

2. Coso Geothermal Field

In this section, we describe the existing geothermal field at China Lake, California. A thermodynamic model is developed using IPSEpro software, and constraints on the system design are discussed.

2.1 Description of existing geothermal field and theoretical model

The Coso geothermal field is located within the Naval Air Weapons Station (NAWS), China Lake, California, and is operated by the Coso Operating Company (COC). The power-generating facility at Coso consists of four geothermal power plants that have a total of nine 30 MW_e turbine-generator units, with a rated capacity of 270 MW_e. The units were constructed by Mitsubishi and Fuji between 1987 and 1990. The power plants use double-flash technology and are supplied with fluid from 80 to 90 production wells. The wells are interconnected to enable the plant to divert captured steam to the appropriate individual turbine generator sets. Some 30 to 40 injection wells can be used to balance the steam field conditions. Produced fluids are moderately saline chloride brines with total dissolved solids from 7,000–18,000 ppm. Non-condensable gases account for 6% of the gas fraction, with 98% of that from CO_2. Hydrogen sulfide ranges from <10–85 ppm.

Table 1 shows the design operating conditions for a single turbine unit. Operational data from COC indicate that each turbine currently produces 8.4 MW (28 %) less power than it was designed to. The current mass flow rate of steam is similar to the design case, and the power loss is mainly the result of reduced steam pressures and temperatures.

Table 1: Design parameters of the 30 MW_e Fuji turbine unit installed at Coso

		High-pressure turbine stage	Low-pressure turbine stage
Mass flow	kg s^{-1}	47.8	72.4
Temperature	°C	163.0	111.0
Pressure	bar	6.3	1.4
Gross power	MW_e	30.0	

A model of the geothermal plant was developed using IPSEpro simulation software (SimTech 2017). IPSEpro is commercial software capable of modelling thermodynamic cycles at design and off-design conditions. The Coso geothermal plant has a large number of inputs, components, and interconnected processes. In this analysis, the power plant is simplified to a single turbine unit with a single production fluid input, steam production from two flash tanks, and a two-stage (high-pressure and low-pressure) turbine. The production fluid enters a high-pressure flash tank (HP FT), and the steam fraction enters the high-pressure stage of the steam turbine. The brine fraction is diverted into the low-pressure flash tank (LP FT), and the generated lower-pressure steam enters the low-pressure stage of the turbine.

The design operating point of the system was established using the design values given in Table 1. Pressure drops in the flash tanks and pipes were approximated using measured values provided by COC. An off-design model was then implemented. The current operating point was modelled by setting the turbine inputs to values that are representative of the current performance. Table 2 shows input and output values from the IPSEpro model, and these values were found to give good agreement with measured data.

Figure 1 shows the off-design performance of the modeled turbine unit. The turbine is currently operating at a gross power of 22.5 MW_e and a net power of 21.7 MW_e, which corresponds to an efficiency of 13.7%. The objective of the hybridized turbine is to increase the power production by 4 MW_e to 25.7 MW_e, corresponding to an efficiency of 14.9%. (Note, this value does not include the additional heat input from the solar field, which is necessary to calculate the hybrid plant efficiency).

Table 2: Design and off-design inputs and performance data used in the IPSEpro model of a single turbine at the Coso geothermal field

		Design conditions		**Current operating conditions**	
		High pressure	*Low pressure*	*High pressure*	*Low pressure*
Mass flow	kg s^{-1}	48.0	25.0	48.0	14.3
Temperature	°C	169.2	132.5	163.4	126.1
Inlet pressure	bar	6.3	1.4	5.7	0.9
Gross power	MW_e	30.0		22.5	
Net power	MW_e	29.2		21.7	
Condenser load	MW_{th}	161.2		164.6	
Efficiency	%	15.6		13.7	

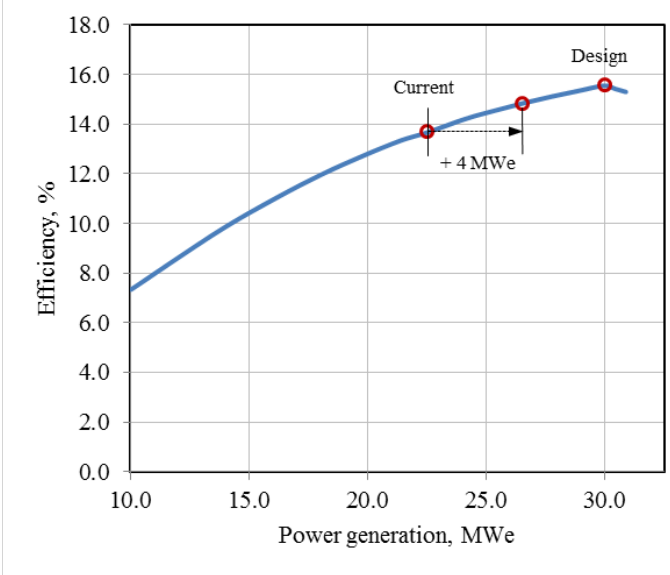

Figure 1: Variation in efficiency with load for the modeled Coso geothermal power plant turbine, as calculated by the ISPEpro model.

2.2 Constraints on the hybrid system design

There are a number of practical constraints on the future hybrid design. The primary objective of the hybridization is to augment electrical power production by 4 MW_e. This objective can be achieved by adding solar heat to the system. The solar heat could be added in several locations, such as to the production well fluids or to the steam entering the turbine. The former is unsuitable because the production fluids are two-phase, which would complicate the design and operation of the heat exchanger. The latter was ruled out because the steam is at a similar temperature to the turbine design value, so increasing the mass flow rate or pressure would have a more significant impact.

Alternatively, solar heat could be added to the condenser water or the brine fraction from the second flash tank. In the latter method, a fraction of the brine is heated by a solar fluid in a heat exchanger, and it is subsequently mixed with the incoming production fluids. The mixture then passes through the two flash tanks as normal. This approach has several practical advantages. For example, the brine is already pumped to a pressure of 15–20 bar so that it can be injected into the geothermal field. It can therefore be heated to a high temperature without requiring additional pressurisation. In addition, the flash tanks and pumps of the Coso plant are close to the proposed location for the solar field, so the brine will not have to be pumped long distances. On the other hand, only a fraction of the brine that the solar field heats is flashed into steam; the remainder is re-injected. As a result, the solar field will be larger than if steam were generated directly.

Heating the condenser water is an attractive option because steam can be generated without the risk of scaling in the heat exchanger. Because all of the solar heat generates steam which enters the turbine, the solar field is smaller than the approach where injection brine is recirculated. However, water is a sparse resource at the Coso field and is continually lost due to evaporation. Additional make-up water is required to provide sufficient cooling. Heating the condenser water would increase the demand for make-up water, and consequently, the most practicable option is to heat a fraction of the injection brine.

The quantity of brine that is recirculated should be limited to around 20%–30% of the injection brine to avoid significant scaling in the pipes and heat exchangers. To prevent production wells from being suppressed, the recirculated brine pressure is constrained to be below 20 bar. Furthermore, to reduce scaling in the heat exchanger and to avoid additional complications, the brine should remain in the liquid phase. The maximum pressure of 20 bar corresponds to a saturation temperature of 207°C.

3. Solar hybrid plant design

In this section, the hybrid design is developed, and the influence of key design variables is investigated.

3.1 Potential plant configurations

Given the constraints listed above, two practical plant designs are illustrated in Figure 2 and Figure 3. These systems heat a fraction of the injection brine, which is then mixed with the production fluids. Figure 2 shows a system where energy is stored directly in the thermal oil. This scheme requires two tanks and a large fluid inventory. To reduce the cost of storage, a heat-transfer fluid with a low cost, high volumetric heat capacity and low vapor pressure is required.

An alternative scheme that uses a thermocline storage tank, such as a packed bed, is shown in Figure 3. This approach may be more economical because it requires only one storage tank, which may be relatively compact because pebbles typically have higher volumetric heat capacities than thermal oils. On the other hand, thermodynamic losses in the thermocline may be significant and these systems require detailed analysis and careful design.

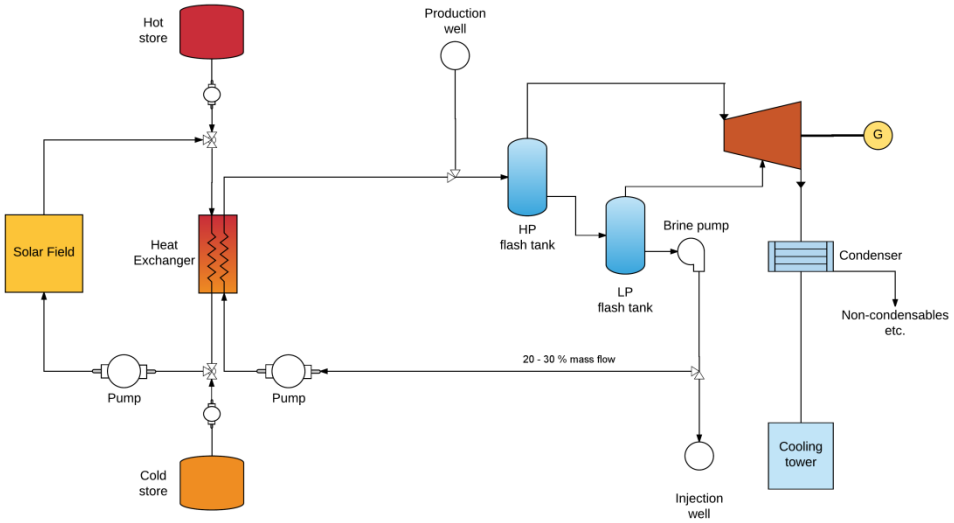

Figure 2: Schematic diagram of the hybrid geothermal-solar power plant with two-tank storage of oil.

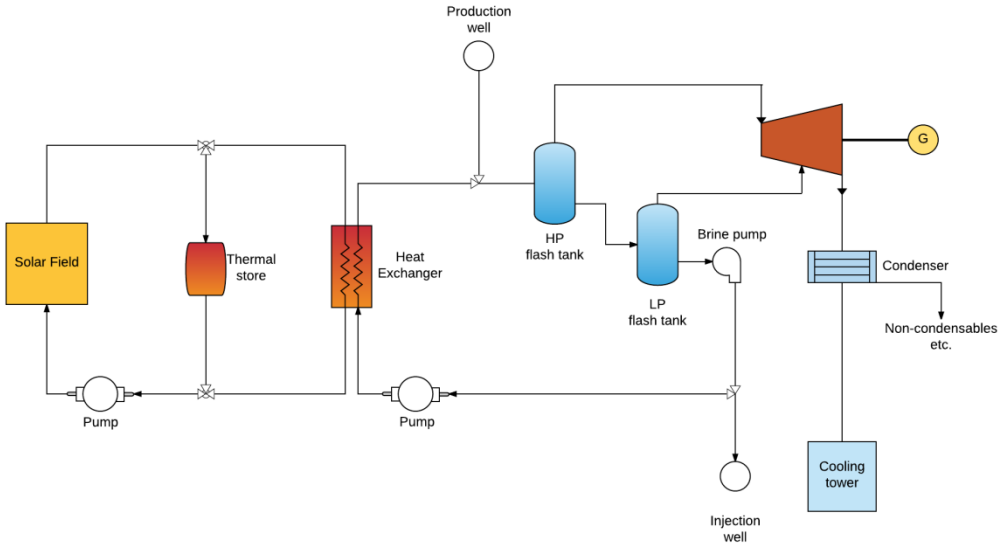

Figure 3: Schematic diagram of the hybrid geothermal-solar power plant with a thermocline storage system.

3.2 Influence of design variables on system performance

The design values that can be varied are the fraction of injection brine that is recirculated, the temperature to which the brine is heated, and the way in which the flash tanks are operated. Recirculating brine increases the enthalpy of the input brine to the flash tank, thereby increasing the mass flow rates and pressure of the output steam. There are two operating strategies to be investigated:

1. Constant-pressure operation: the pressure drop in the flash tank is held constant, thus increasing the steam mass flow rate.
2. Sliding-pressure operation: the steam mass flow rate is held constant, thus increasing the steam pressure.

In practice, it is likely that the steam output will be somewhere between these two extreme cases, depending on how the flash tanks and input fluids are controlled.

Recirculating the injection brine leads to an increase in the power generation under both operating strategies as shown in Figure 4. Power increase is more significant in the sliding-pressure operation than in the constant-pressure operation, because mass flow rates are closer to design conditions than operating pressures. The power increase in the low-pressure stage levels off at a solar heat addition of around 20 MW_{th}. When the outlet of the high-pressure turbine and the low-pressure flash tank mix, the fluid assumes the lowest pressure of the two streams before it enters the low-pressure turbine. The high-pressure turbine exhaust steam has a fixed pressure of 1.4 bar, and this is the maximum pressure that can enter the LP stage. At current operation, the exit pressure of the LP FT is around 0.9 bar. Increasing this pressure significantly increases the power output. However, there reaches a point where pressure from the low-pressure flash tank exceeds 1.4 bar for the first time, and this additional pressure is not utilized.

The temperature of solar-heated brine has a significant impact on the power output as illustrated in Figure 5. As expected, higher temperatures lead to higher power output. It is notable that there is a brine temperature that leads to lower power output than the current operation of 22.5 MW_e, even though the enthalpy into the flash tanks has increased. Mixing the recirculated brine with the production fluids reduces the steam fraction of the two-phase brine. Thus, for a given flash-tank pressure drop, the mass fraction of steam is reduced. On the other hand, for a given steam mass flow rate, a larger pressure drop is required. Both of these factors lead to a reduced power output. This analysis suggests that the brine should be heated to over 155°C to increase the power output.

3.3 Selection of a baseline hybrid design

Based on the investigations of section 3.2, a baseline hybrid design with a power boost of 4 MW_e is configured. The input variables are given in Table 3. This design increases both the steam mass flow rate and pressure that exit the flash tanks, which is more realistic than keeping one of these variables constant. This baseline design will be used to investigate the sizing of the solar field and the thermal storage.

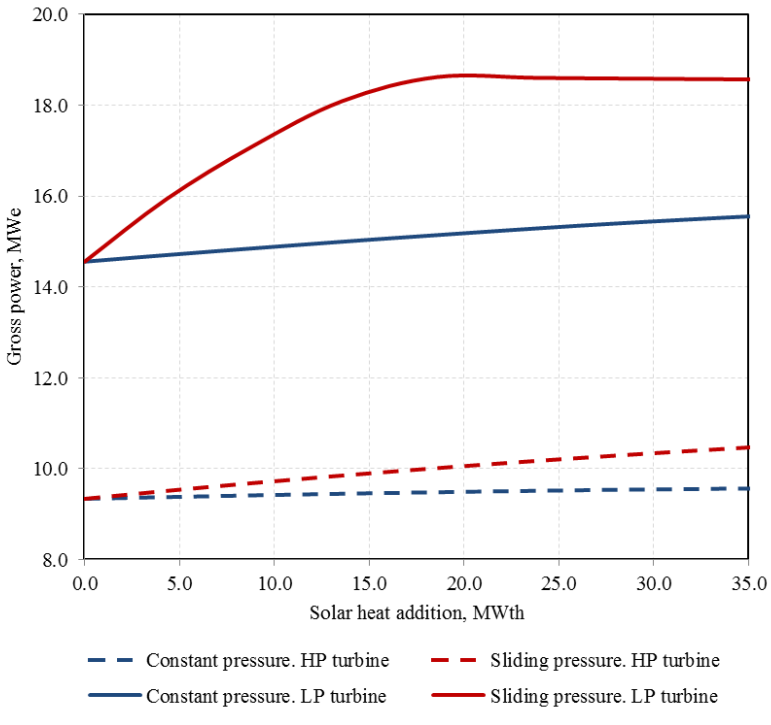

Figure 4: Impact of increasing the solar heat addition on the turbine power output. Solar heat addition is controlled by varying the recirculated brine mass flow rate.

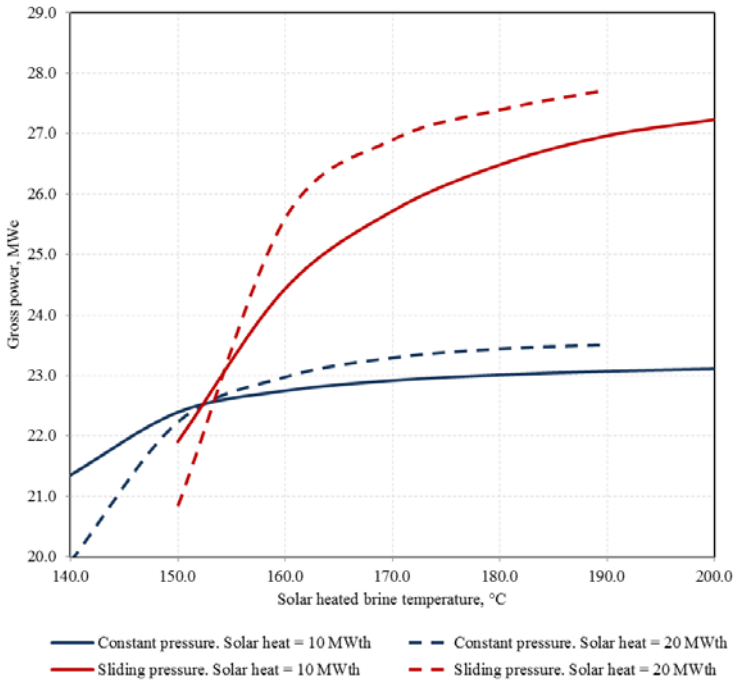

Figure 5: Influence of the recirculated brine temperature on turbine power output. The solar heat addition is constant along each curve.

Table 3: Baseline hybrid design with a power boost of 4 MW_e

		High-pressure turbine stage	Low-pressure turbine stage
Mass flow	kg s^{-1}	49.0	64.4
Temperature	°C	165.1	106.4
Pressure	bar	6.0	1.27
Net power	MW_e	25.7	
Condenser load	MW_{th}	142.1	
Efficiency	%	15.6	
Solar-heated brine			
Mass flow	kg s^{-1}	73.7	
Pressure	bar	20.0	
Temperature into HX	°C	131.2	
Temperature out of HX	°C	180.0	
Thermal input	MW_{th}	15.6	
Increase in net power	MW_e	4.0	
Solar conversion efficiency	%	25.6	

4. Solar collector design

Hyperlight Energy, with its development partner, NREL, is funded under the U.S. Department of Energy (DOE) SunShot Initiative and the California Energy Commission to develop a low-cost CSP solution. Hyperlight Energy has developed an advanced linear Fresnel reflector based on repurposed agribusiness materials (e.g., water and plastic). These low-cost materials have demonstrated lifetimes of over 25 years in environments that are comparable to those in which Hyperlight products will ultimately be deployed – i.e., intense solar, intense heat, low humidity, blowing abrasive dust, and rodent and insect infestation. The Hyperlight team is focusing its solar thermal plant design on a scale that both supports rapid iterative product development, and factory production/deployment operations of "kits" that can be quickly produced and field-deployed with minimal required construction resources. Hyperlight is aiming to achieve an installed capital cost of <\$100/m^2 reflector aperture by 2017 with a target of \$50/m^2 reflector aperture by 2020.

4.1 Hyperlight collector system

A Hyperlight Energy solar thermal plant consists of an array of sealed water basins that support and constrain the vertical positioning accuracy of a "raft" collector system (Figure 6). These heavy (~25 tonne) water beds mitigate the impacts of strong winds on the optical performance of the collector. The "raft" collector provides sufficient pointing accuracy of a linear beam of light incident on a suspended hot oil loop to ensure that over the lifetime of the product, the thermal power production remains within 95% of beginning-of-life operations.

The Hyperlight collector will initially be deployed in commercial/industrial process-heat applications (<1 MW_{th} typical) as early as 2018, with a slightly longer-term objective of supporting much larger-scale (10s of MW_{th}) geothermal hybridization applications post-2018. In 2017, IAPMO (International Association of Plumbing and Mechanical Officials) certification of a 0.5 acre (16 basins) of the Hyperlight collector will be completed at a pilot site in Brawley, CA. This certification process is a prerequisite to qualifying for the California Solar Initiative Thermal Program (CSITP) that subsidizes natural gas displacements with solar thermal power. The 0.5 acre pilot site will also support additional early-stage pilot testing of CSP process-heat applications, including a reduced-scale hybrid plant such as that described in this paper. To date, Hyperlight has undertaken accelerated lifecycle testing, which simulated 25+ years of operation on a representative "raft" opto-mechanical system with introduced contamination as part of the DOE SunShot Initiative.

A summary of performance parameters for the Hyperlight CSP product is provided in Table 4 and Table 5.

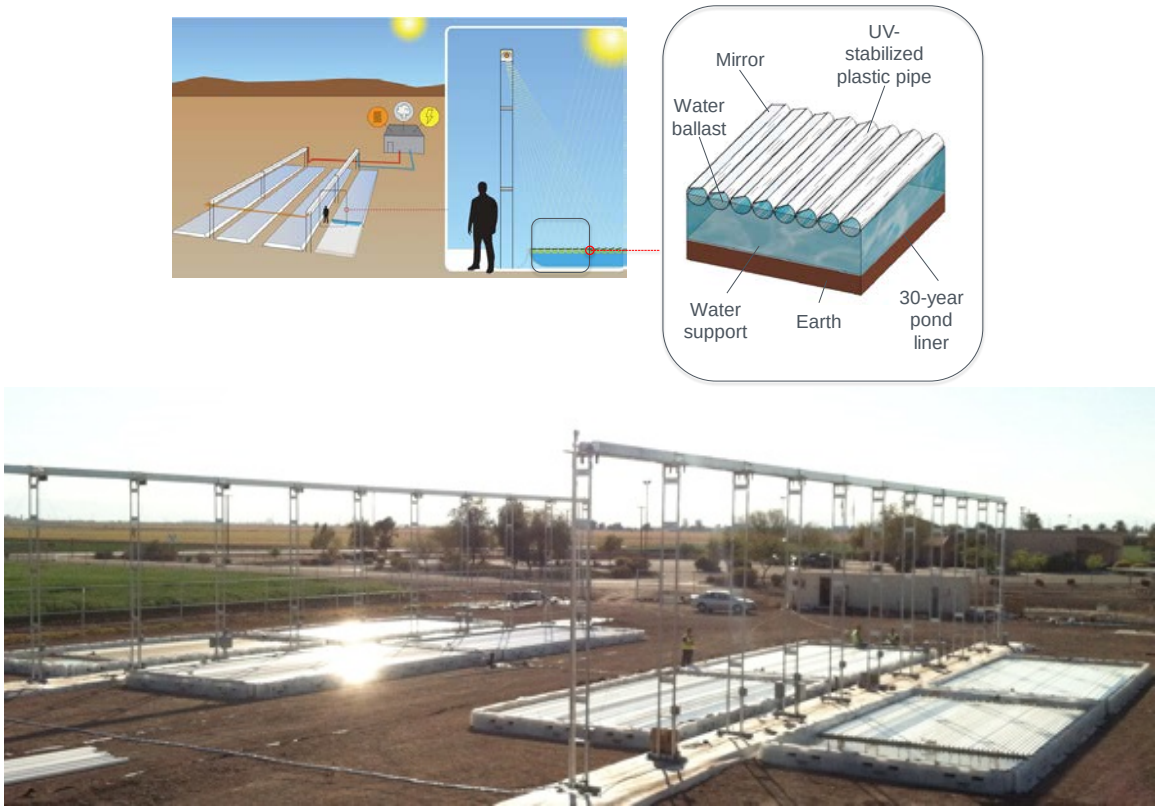

Figure 6: Hyperlight CSP plant based on waterborne linear Fresnel reflector collector system.

Table 4: Summary of baseline collector geometry

Attributes		Value
Total collector width	m	13.7
Total collector effective width (W_{field})	m	12.2
Net reflector aperture width ($W_{primary}$)	m	9.9
No. of basins along width		2
Basin width	m	6.1
Basin length	m	15.2
No. of reflectors per basin		50
Active primary mirror aperture area per basin pair	m^2	144.9
Active primary mirror aperture as % of collector width footprint	%	66.0
Absorber tube design height	m	7.5 ± 0.5
Absorber tube optimal design diameter	mm	90.0

Table 5: Summary of modeled optical properties for baseline collector and baseline receiver

Attributes		Value
Collector Primary Reflector		
Reflectance of primary mirror		0.94
Primary mirror specularity	mrad (Gaussian)	1.50
RMS of all collector optomechanical errors, primary mirror slope error, and receiver alignment + deflection errors	mrad (Gaussian)	3.00
Receiver Secondary Reflector		
Reflectance		0.94
Specularity	mrad (Gaussian)	1.50
Slope error	mrad (Gaussian)	2.00
Receiver Heat Collecting Element (HCE)		
Anti-reflection coatings		Yes
Transmittance of outer glass shell		0.97
Thickness of outer glass shell	mm	3.00
Absorptance of absorber tube		0.96

5. Sizing of solar field and thermal storage

Having established a baseline hybrid design that increases the power output by 4 MW_e, the solar field and thermal storage can be sized accordingly. The thermal power that the solar field should provide under design conditions is equal to the thermal input to the recirculated brine and is 15.6 MW_{th} (see Table 3). The heat-transfer fluid is assumed to be a synthetic oil with properties similar to Therminol VP-1 or Dowtherm A. These oils are popular options in CSP plants and comprise a eutectic mixture of biphenyl and diphenyl oxides. The temperature difference between the solar oil and the recirculated brine in the heat exchanger is assumed to be 50°C. Given the required power and the temperatures, the mass flow rate of solar HTF is calculated.

To determine the solar-field design, the design condition is first defined as the peak solar irradiance at China Lake on the summer solstice. TMY3 solar data for China Lake were obtained from NREL's System Advisor Model (NREL 2017). The collector conversion efficiency was calculated for each hour of the year by taking into account the sun angle, optical and thermal efficiencies of the Hyperlight collectors, and spacing between the collectors (the mirror aperture is about 60% of the land area). It was calculated that a design-point direct normal irradiance (DNI) of 950 W m^{-2} at the summer solstice day is converted into 555 W m^{-2} of thermal power by

the collectors. Based on these figures, the area of a solar field with a solar multiple of 1 is 28,012 m^2.

"Solar multiple" is defined as the ratio between the actual solar-field size and the required size to produce the design power output at the peak DNI on the summer solstice. Increasing the solar multiple above 1 proportionately increases the size of the solar field, the HTF mass flow rate, and therefore, the thermal power. The maximum power delivered by the solar field to the heat exchanger is fixed at 15.6 MW_{th}, and any excess energy can be either stored or curtailed when the storage is fully charged. The energy capacity of the storage is found by choosing the duration of storage and assuming that the storage can discharge at the nominal power of 15.6 MW_{th} for this duration. If the storage is fully charged and there is available solar energy, then the additional power could either be delivered directly to the hybrid system or it could be curtailed. The former option is preferable, and it is likely to increase the additional power generation beyond 4 MW_e.

Two types of storage are considered in this paper. The first—direct storage of the thermal oil in pressure vessels—requires two storage tanks, as in Figure 2. The second approach is thermocline storage, which requires only one storage tank, as in Figure 3. The thermocline storage could consist of a packed bed of pebbles or a series of tubes through a concrete matrix. If a two-tank storage solution is used, then the mass of HTF in the storage tank is given by the duration of storage multiplied by mass flow rate of HTF out of the storage tank during discharge. Both storage tanks should be large enough to accommodate this mass of HTF plus an additional 20% safety factor. On the other hand, a packed-bed storage tank is sized using the following equation:

$$E = \alpha V \left\{ \rho_s \left(1-\varepsilon\right)\left(cT\big|_s^H - cT\big|_s^C \right) + \varepsilon \left(\rho cT\big|_L^H - \rho cT\big|_L^C \right) \right\}, \tag{1}$$

where E is the energy stored, V is the volume, ρ is the density, c is the specific heat capacity, T is the temperature, and ε is the fraction of the storage tank taken up by oil. Subscript L refers to the oil and s to the solid pebbles; superscripts H and C refer to the conditions at the hot and cold states, respectively. The factor α accounts for the shape of the thermocline in the storage tank. A value of $\alpha = 1$ indicates that the storage is fully charged. However, the packed bed is unlikely to be operated in this way, because the thermocline would exit the storage tank, leading to significant losses. For the thermocline to be kept within the storage tank requires that a fraction of the volume not be utilized. In this study, α is set to 0.75.

Having sized the solar field and the thermal storage, the power output and storage behavior is calculated for every hour of a representative year. For a solar multiple of 1 over the course of a year, the solar field only occasionally produces the required thermal power of 15.6 MW_{th} and storage is unnecessary. To provide the required power during the winter or into the evenings, the solar multiple is increased. Solar multiples of 2.4 and 3.9 were considered with storage durations of 4 and 8 hours. System design parameters and performance data are shown in Table 6.

Figure 7(a) and Figure 7(b) show the power output for three days around the summer and winter solstice, with a solar multiple of 2.4 and thermal storage duration of 8 hours. Figure 7(a) indicates that during the summer, the solar field is able to provide the required power, as well as charging the thermal storage and delivering a substantial quantity of power in the evenings. There is a small quantity of excess energy that could be avoided with more storage.

Alternatively, the excess power could also be added to the geothermal field, thus further increasing the power output. During the winter, the solar field rarely delivers the required 15.6 MW_{th} of power, and the storage has a very low capacity factor. Over the course of the full year, the average power delivered by the solar field including storage is 7.7 MW_{th}, which corresponds to a capacity factor of 49.8%.

This suggests that larger solar multiples are required to provide sufficient power during the winter. Figure 7(c) and Figure 7(d) show the power output for a solar field with a solar multiple of 3.9 and a storage duration of 8 hours. The quantity of excess solar heat substantially increases, with around 24.9% of the solar heat generated being surplus to requirements. However, the storage is used to a greater extent and is frequently fully charged during the summer. In addition, the power production during the winter increases and the capacity factor increases to 66.8%.

Consequently, it can be seen that a large solar multiple is necessary to provide the required power throughout the year. However, this leads to larger solar fields and excess energy during the summer. If the excess energy can be used in the geothermal plant, then this is advantageous. If there are practical constraints on the quantity of excess energy that can be delivered, then larger thermal storage tanks could be installed. However, large storage tanks will be underutilized during the winter and are more likely to be uneconomical.

Alternatively, it may be preferable to design a system that has a small solar field, and shorter-duration storage that is capable of producing power only at peak-demand times such as the rapid increase in energy demand associated with California's "duck curve" during early evening hours (Denholm *et al.* 2015). These alternative strategies should address the technical issues associated with the rapid increase in power and the ramp rates that would be required. A detailed economic analysis is ultimately required to determine what sizing may be most economically beneficial relative to the cost and technical challenges.

The choices of heat-transfer fluid and storage technology are important parameters and determine the thermodynamic performance as well as the economic feasibility of the plant. It is notable that the volumes of each of the two-tank stores are about three times the size of the packed bed, as a result of pebbles having a volumetric heat capacity roughly five times greater than oil. The ultimate decision will be based on the cost and technological maturity. Other properties of interest are the operating temperature range (larger temperature ranges lead to smaller stores at the cost of managing higher temperature heat), volumetric heat capacity (larger heat capacities lead to smaller stores), vapor pressure (lower vapor pressures reduce the need to pressurize the system, which would significantly increase the system cost), and viscosity, which correlates to pumping power. The thermal stability of the fluid and its toxicity or environmental impact must also be considered. Oxidation of the thermal fluid is particularly important because the heat-transfer fluid is likely to be at high temperatures and there will be contact between the fluid and air in the storage tanks. Oxidation will reduce the thermal performance of the fluid and will increase its viscosity, thereby requiring it to be replaced more frequently.

Table 6: Main results of sizing the solar field and thermal storage for the cases with 4 and 8 hours of storage. Two storage systems are considered: TT—two-tank direct storage of oil; PB—one-tank thermocline packed bed.

Solar-field sizing		4 hours of storage		8 hours of storage		8 hours of storage	
Required power	MW_{th}	15.6		15.6		15.6	
Solar multiple	-	2.4		2.4		3.9	
Design solar power	MW_{th}	39.6		36.9		60.8	
Solar field area	m^2	67 170.0		67 170.0		110583.1	
Solar field area	acres	16.6		16.6		27.3	
Peak HTF mass flow	kg s^{-1}	233.8		233.8		384.9	
Thermal storage sizing		TT	PB	TT	PB	TT	PB
Hot-storage volume	m^3	1912.4	625.6	3827.9	1251.2	3824.9	1250.2
Cold-storage volume	m^3	1830.0		3663.1		3660.2	
Energy storage	MWh	62.2		124.4		124.4	
Hours of storage	h	4.0		8.0		8.0	
Performance							
Total solar input	GWh	331.8		331.8		546.3	
Total thermal energy	GWh	68.4		68.4		112.6	
Energy produced	GWh	59.7		67.8		84.5	
Excess energy	GWh	8.7 (12.7%)		0.6 (0.82%)		28.1 (24.9%)	
Efficiency *	%	18.0		20.4		15.5	
Average power	MW_{th}	6.8		7.7		9.6	
Capacity factor	%	43.8		49.8		62.0	
Average storage discharge	MW_{th}	10.3		11.8		13.4	
Average discharge duration	h	4.0		5.6		6.3	
Utilization of storage	%	63.1		49.5		74.5	

* Efficiency does not include excess energy that could be supplied to the geothermal plant

6. Conclusions and further work

Retrofitting a geothermal plant with CSP and thermal storage can increase the power output. Such a system has the potential to reduce the total cost of delivered electricity and better tailor power production to actual grid demand. A thermodynamic model of the Coso geothermal power plant was developed, and practical constraints were considered to develop a practical hybrid design. The Coso turbine unit operates 7.5 MW_e below its 30 MW_e design capacity and a solar hybrid system aims to augment the power by 4 MW_e.

It was found that the sliding-pressure operation strategy is able to produce more power than the constant-pressure strategy with the same solar heat input. The brine should be heated to at least 155°C to increase the power production, although it is constrained to a maximum temperature of 207°C by practical constraints.

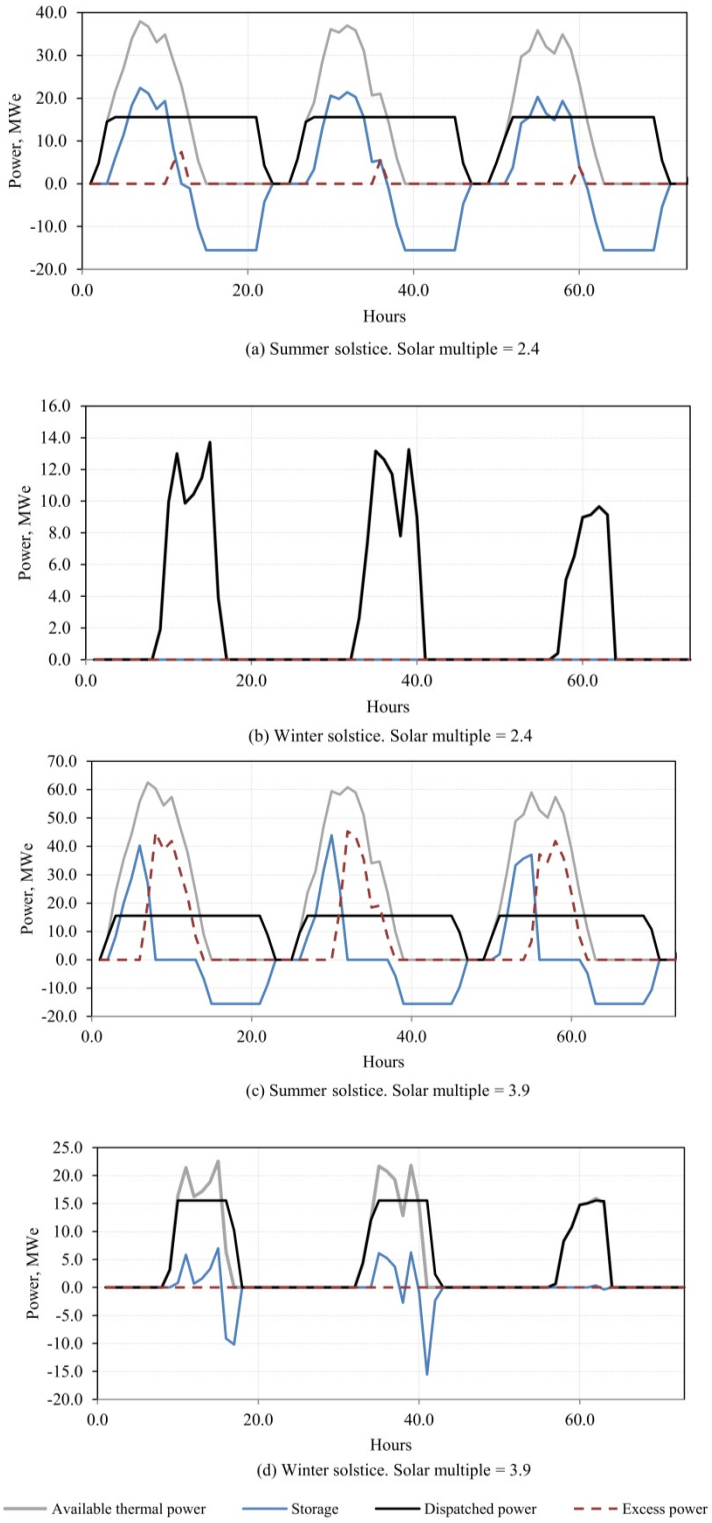

Figure 7: Time-series comparing the solar output for the summer and winter solstice and the two days either side. Sub-figures (a) and (b) have a solar multiple of 2.4 and sub-figures (c) and (d) have a solar multiple of 3.9. Both cases have 8 hours of thermal storage. Full details and results are given in Table 6.

The effect of different solar multiples and storage durations on the sizing and performance of the solar field were considered. It was found that low solar multiples led to a hybrid plant that was unable to provide the required power throughout the winter. In addition, storage was under-utilized. By increasing the size of the solar field, the hybrid plant can provide the required 15.6 MW_{th} for more than 60% of the year. However, further work is required to determine the economic feasibility of such a system and to investigate whether it would be more advantageous to provide smaller quantities of energy at times of peak demand.

Future research will consider a range of storage technologies and heat-transfer fluids. If a two-tank storage system is used, then large volumes of heat-transfer fluid will be required and factors such as cost, heat capacity, and vapor pressure will be influential. In this paper, it was shown that packed beds are roughly six times smaller (in total) than a two-tank method and are therefore potentially more economical. Maturity and availability of different thermal storage technologies will be evaluated before the final selection.

The time-series analysis in this paper should also be extended to consider how the turbine unit performance varies throughout the year. For instance, as the power delivered by the solar field varies during the day, the mass flow rate or temperature of the recirculated brine will change, thereby affecting the off-design performance. Furthermore, the impact of ambient temperatures on the system performance will also be investigated.

Acknowledgements

The work was supported by the U.S. Department of Energy under Contract No. DE-AC36-08GO28308 to the National Renewable Energy Laboratory (NREL). The authors gratefully acknowledge the support and contributions of the Naval Geothermal Program Office, including Andrew Sabin, David Meade, Michael Lazaro and Kelly Blake.

Nomenclature

Acronyms

COC		Coso Operating Company
CSP		Concentrating solar power
DNI	W m^{-2}	Direct normal irradiance
FT		Flash tank
HTF		Heat-transfer fluid
HP		High pressure
HX		Heat exchanger between the solar field and the recirculated brine
LFR		Linear Fresnel reflector
LP		Low pressure
NAWS		Naval Air Weapons Station
PB		Packed-bed thermocline storage system
SAM		System Advisor Model
TMY		Typical Meteorological Year
TT		Two-tank storage system using thermal oils

Roman letters

c	kJ kg^{-1} k^{-1}	Specific heat capacity
E	J	Energy capacity of storage
T	K	Temperature
V	M^3	Volume

Greek letters

ε		Void fraction
ρ	kg m^{-3}	Density

Subscripts and superscripts

s	Storage
L	Heat-transfer fluid
C, H	Cold and hot temperatures of the storage

References

Alvarenga, Y., Handal, S. & Recinos, M., 2008. Solar steam booster in the Ahuachapan geothermal field. *Geothermal Resources Council 32nd Annual Meeting*, 32.

Ayub, M., Mitsos, A. & Ghasemi, H., 2015. Thermo-economic analysis of a hybrid solar-binary geothermal power plant. *Energy*, 87, pp.326–335.

Denholm, P. et al., 2015. Overgeneration from Solar Energy in California : A Field Guide to the Duck Chart. Available at: http://www.nrel.gov/docs/fy16osti/65023.pdf.

Dimarzio, G. et al., 2015. The Stillwater Triple Hybrid Power Plant: Integrating Geothermal, Solar Photovoltaic and Solar Thermal Power Generation. In *Proceedings World Geothermal*

Congress. pp. 1–5.

Handal, S., Alvarenga, Y. & Recinos, M., 2007. Geothermal steam production by solar energy. *Geothermal Resources Council 31st Annual Meeting*, 31.

Lentz, A. & Almanza, R., 2006. Solar – geothermal hybrid system. *Applied Thermal Engineering*, 26, pp.1537–1544.

Miguel Cardemil, J. et al., 2016. Thermodynamic evaluation of solar-geothermal hybrid power plants in northern Chile. *Energy Conversion and Management*, 123, pp.348–361.

NREL, 2017. System Advisor Model (SAM version 2017.1.17). Available at: https://sam.nrel.gov/.

SimTech, 2017. Process Simulation Environment (IPSEpro version 7.0). Available at: http://www.simtechnology.com/CMS/index.php/ipsepro.

Wendt, D.S. & Mines, G.L., 2015. Stillwater hybrid geo-solar power plant optimization analyses. *Geothermal Resources Council 39th Annual Meeting*, 39, pp.891–900.

Zhou, C., Doroodchi, E. & Moghtaderi, B., 2013. An in-depth assessment of hybrid solar – geothermal power generation. *Energy Conversion and Management*, 74, pp.88–101.

Zhu, G. & Turchi, C., 2017. Solar Field Optical Characterization at Stillwater Geothermal / Solar Hybrid Plant. *Journal of Solar Energy Engineering*, 139(June), pp.1–10.